

Analysis of free vibration in bi-directional power law-based FG beams employing RSD theory

Nafissa Zouatnia¹, Lazreg Hadji^{1,2}, Hassen Ait Atmane³, Mokhtar Nebab^{*3,4},
Royal Madan⁵, Riadh Bennai³ and Mouloud Dahmane⁶

¹Department of Civil Engineering, University of Tiaret, BP 78 Zaaroura, Tiaret, 14000, Algeria

²Laboratory of Geomatics and Sustainable Development, University of Tiaret, Algeria

³Laboratory of Structures Geotechnics and Risks, Department of Civil Engineering,
Hassiba Benbouali University of Chlef, Algeria

⁴Department of Civil Engineering, Faculty of Technology, University of M'Hamed BOUGARA Boumerdes,
Algeria

⁵Department of Mechanical Engineering, Graphic Era (Deemed to be University),
Dehradun 248002, Uttarakhand, India

⁶Ecole National Supérieur D'hydraulique, Blida, 09000, Blida, Algeria

(Received January 17, 2024, Revised July 9, 2024, Accepted July 18, 2024)

Abstract. The present study aims to investigate the free vibration of bi-directional functionally graded (BDFG) beams using a refined shear deformation (RSD) theory. Power law variation of material composition was considered along thickness and longitudinal directions. The beams are considered simply supported. The methodology adopted is the Hamilton principle and the governing equation was solved using Navier's method for simply supported boundary conditions. A metal-ceramic combination of materials was used to provide gradation as per power law variation. The equivalent elasticity modulus and density of BDFG were computed using the rule of mixture. The results of the study were related to published works and found to be a good match. The effect of grading parameters in the thickness and longitudinal direction was studied to investigate its impact on the natural frequency.

Keywords: BDFG beams; free vibration; Hamilton principle; refined shear deformation theory

1. Introduction

Functionally graded materials (FGMs) are materials in which the properties vary gradually through directions. The change in the properties is a result of a change in composition, microstructure gradient, or porosity (Sankar 2001, Avcar 2019, Hadji and Avcar 2020). However, a change in composition type is mostly fabricated. Functionally graded materials have more strength than classical composites and the problem of low strength or delamination can be avoided because of the gradual variation of material properties. FGMs have been specifically designed to work in severe thermal environments because of the presence of ceramics in them. Lezgy-

*Corresponding author, Ph.D. Student, E-mail: nebmokhtar@gmail.com

Nazargah *et al.* established a groundbreaking approach by developing a refined high-order global-local theory for analyzing laminated composite beams. This theory offers a powerful tool for investigating bending, vibration, and even progressive failure analysis (Lezgy-Nazargah *et al.* 2011, Beheshti-Aval and Lezgy-Nazargah 2012, Lezgy-Nazargah 2017, Benkhellat *et al.* 2021, Ghouilem *et al.* 2022) Further extending this framework, in Lezgy-Nazargah (2015), introduced the NURBS isogeometric FE approach to analyze the thermo-mechanical behavior of bi-directional FG beams. The free vibration of a simply supported FG beam was explored using classical beam theory and higher-order theories, the study demonstrates that CBT yields higher values (Aydogdu and Taskin 2007). A state space technique was used to solve the problem of a graded beam resting on the Winkler–Pasternak foundation (Ying *et al.* 2007). Non-linear transient vibration analysis of the BDFG beam was studied by employing Galerkin’s scheme. Though, the vibration modes are both symmetric and asymmetric, an asymmetric material distribution yields asymmetric modes (Lu and Chen 2020). Finite element analysis, SDT, and modified SDT were used to perform dynamic analysis of a beam (Şimşek 2009, Thai and Vo 2012, Ould Larbi *et al.* 2013, Nguyen *et al.* 2017, Benaberrahmane *et al.* 2021, Kehli *et al.* 2024, Ait Atmane *et al.* 2021, Bennai *et al.* 2022, Latroch *et al.* 2023, Mellal *et al.* 2023, Nebab *et al.* 2023, Dahmane *et al.* 2024, Mokhtar *et al.* 2024, Nebab *et al.* 2024). Benfarhat *et al.* (2016) developed a free vibration analysis of FG plates resting on the elastic foundation based on the neutral surface concept using higher-order shear deformation theory. Ayache *et al.* (2018) analyze the wave propagation and free vibration of the functionally graded porous material beam with a novel four-variable refined theory. Fenjan *et al.* (2020) provided a review of a numerical approach for the dynamic response of strain gradient metal foam shells under constant velocity moving loads. Singh and Kumari (2020) used an analytical free vibration solution for the angle-ply piezo laminated plate under cylindrical bending by employing a piezo-elasticity approach. Rabahi *et al.* (2021) developed modeling and analysis of the imperfect FGM-damaged RC hybrid beams. Recently, Lahdiri and Kadri (2022) studied the free vibration behavior of multi-directional functionally graded imperfect plates using a 3D isogeometric approach. Frahlia *et al.* (2023), studied the vibration response of an FG plate resting on a viscoelastic bed using a high-order shear deformation theory with four unknowns. In recent works (Karamanli *et al.* 2023, Lezgy-Nazargah *et al.* 2023, Lezgy-Nazargah *et al.* 2024), Lezgy-Nazargah *et al.* (2023) continued to push the boundaries of knowledge. They explored the bending, buckling, and free vibration behaviors of various complex beam configurations. These include 2D FG curved beams, bi-directional FG curved sandwich beams, and even shallow-to-deep FG curved sandwich beams. Their studies incorporated sophisticated theories like the global-local refined shear deformation theory.

The fabrication of functionally graded material is characterized as gas-based, liquid-based, and solid-based. Gas-based methods are usually used for coating purposes (Madan and Bhowmick 2020). Centrifugal casting is one of the liquid-based methods in which the reinforcement is added in a molten metal pool thus due to rotation the reinforcement is dispersed along the radius thus, this method is suitable only for axisymmetric objects. Powder metallurgy and additive manufacturing methods are solid-based methods that can be used to fabricate complex geometries. For the fabrication of the FGM disk, a novel powder metallurgy technique was proposed in which a metal-ceramic-based layered FGM was fabricated (Madan and Bhowmick 2022). A similar technique can be used to fabricate a bi-directional FG beam. One of the disadvantages of the layered-based method is the concentration of stresses at the interface of two layers which arises because of the different properties of the two materials. A composition change must be smooth to avoid delamination (Norio *et al.* 1992, Nakamura *et al.* 2000). The change in composition can be

layer-wise or continuous. So, accordingly, a fabrication route is planned. To produce a layer-wise structure powder metallurgy (P/M) method is preferred. However, the layering of composites to form functionally graded materials could cause delamination at the interface. Therefore, an additive manufacturing technique is useful because in this method large number of layers can be created which are of very small thickness (Benoit *et al.* 2021, Ansari *et al.* 2021, Abdalla *et al.* 2021). On the other hand, a centrifugal casting method is said to give continuous distribution of graded material but that too depends on multiple factors like pouring temperature, rotation speed, and others. Also, there will be no control over the change in composition which is best achieved in the P/M process (Akinwamide *et al.* 2020, Verma *et al.* 2021). Theoretically, a variation in composition is provided by changing the composition as power law, exponential law, and others. A change in microstructure is a result of heat treatment and so the properties will change. Porosity has advantages as it can dampen the vibration induced but on the other hand, it also reduces the effective material properties. For functionally graded materials to work under severe thermal environments it is reinforced with ceramics such as alumina, and silicon carbide along with metal-based matrix materials such as aluminum, magnesium, nickel, and steel, etc. To overcome this problem an additive manufacturing technique can be used in which several small layers can be stacked to develop a final component. The larger the number of layers the smaller the stress jump is at the interface. The fabricated samples can be easily tested to confirm the successful fabrication of bi-FGM by performing several metallographic tests to understand the microstructural characterization.

The present study uses an RSD theory to investigate the free vibration of bi-directional functionally graded (BDFG) beams. Power law variation of composition was considered and the rule of mixture was used to define the equivalent material properties. The rule of mixture gives the upper and lower bound values of material properties which means all the other model estimates must fall inside the band. The rule of mixture could not predict the properties of particle composite effectively, but it can be applied for lower ratios of material combinations. Its applicability can be extended in modeling the porosity effects as well. Hamilton’s principle was used in combination with the Navier method. The natural frequency of FG beams was calculated for different grading indices for both longitudinal and thickness directions. Beams have huge industrial applications, therefore the study of the natural frequency is important so that the chances of resonance in which the amplitude is maximum can be eliminated. The fabrication technique is also discussed which will allow the reader to understand composition change in a better way. Also, the research opens up the scope for the fabrication of such materials.

2. Problem formulation

Consider a bi-directional graded beam model of length L , width b , and height h . Assuming the material of the beam consists of two ceramics (designated ceramic-1 and ceramic-2) and two metals (designated metal-1 and metal-2) whose composition varies in longitudinal and thickness directions (Ould Larbi *et al.* 2013).

$$V_{c1} = \left(\frac{z}{h} + \frac{1}{2}\right)^{n_z} \left[1 - \left(\frac{x}{L}\right)^{n_x}\right]$$

$$V_{c2} = \left(\frac{z}{h} + \frac{1}{2}\right)^{n_z} \left(\frac{x}{L}\right)^{n_x}$$

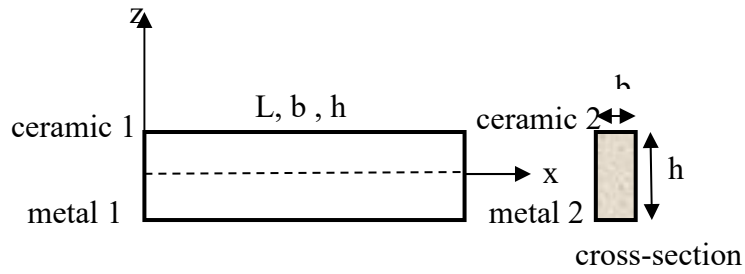


Fig. 1 Geometry and coordinates of BDFG beam

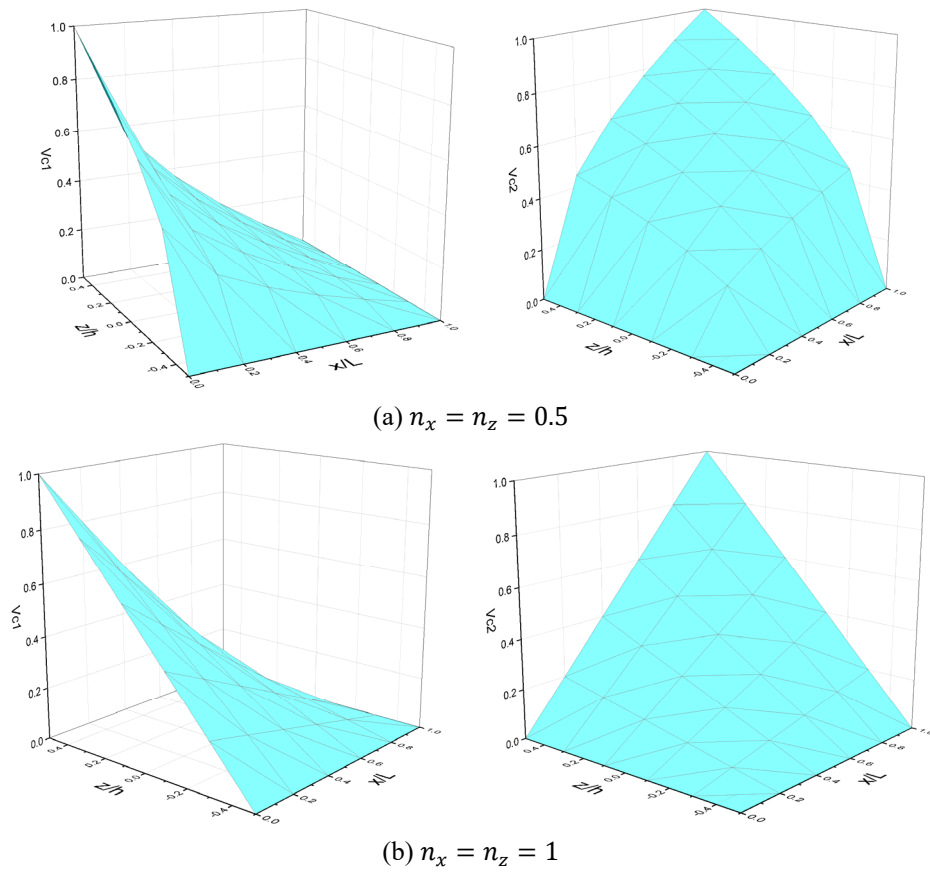


Fig. 2 (a-b) Variation of volume fractions of ceramics in both directions

$$\begin{aligned}
 V_{m1} &= \left[1 - \left(\frac{z}{h} + \frac{1}{2} \right)^{n_z} \right] \left[1 - \left(\frac{x}{L} \right)^{n_x} \right] \\
 V_{m2} &= \left[1 - \left(\frac{z}{h} + \frac{1}{2} \right)^{n_z} \right] \left(\frac{x}{L} \right)^{n_x}
 \end{aligned}
 \tag{1}$$

where n_z and n_x are the grading indices along the thickness and longitudinal directions.

In Fig. 2, the variation of the volume fraction of ceramic 1 and ceramic-2 in both directions is represented for two values of grading indexes n_z and n_x . To model the material such as Young’s modulus and mass density of the BDFG beam Voigt model was used (Benaberrahmane *et al.* 2021). The model is best suited for material combinations for which the ratio of two material properties is less. The model assumes perfect binding between the metal and ceramic and the ceramic reinforcement is in the form of long fibers (Madan et Bhowmick 2021).

$$P(x, z) = \left[(P_{c1} - P_{m1}) \left(\frac{z}{h} + \frac{1}{2} \right)^{n_z} + P_{m1} \right] \left[1 - \left(\frac{x}{L} \right)^{n_x} \right] + \left[(P_{c2} - P_{m2}) \left(\frac{z}{h} + \frac{1}{2} \right)^{n_z} + P_{m2} \right] \left(\frac{x}{L} \right)^{n_x} \tag{2}$$

We note that in Eq. (2) when $n_x = 0$ we will have a unidirectional FG beam with ceramic-2 and metal-2. Moreover, if $n_z = 0$, we will have an axially unidirectional FG beam made from ceramic 1 and ceramic 2.

2.1 Kinematics and constitutive equations

Eq. (3) shows the kinematic relation from which strain and stress were obtained. Initially, the displacement solution was determined, which was then post-processed to obtain the strain and stress induced in the beam.

The displacement field of the refined beam theory is given by

$$u(x, z, t) = u_0(x, t) - z \frac{\partial w_b}{\partial x} - f(z) \frac{\partial w_s}{\partial x} \tag{3a}$$

$$w(x, z, t) = w_b(x, t) + w_s(x, t) \tag{3b}$$

The index b denotes the bending effect, while index s represents the shear effect, this applies to the rest of the equations. In this work, the present refined shear deformation beam theory is obtained by setting

$$f(z) = -\frac{1}{4}z + \frac{5z^3}{3h^2} \tag{4}$$

The strains associated with the displacements in Eq. (3) are

$$\varepsilon_x = \varepsilon_x^0 + z k_x^b + f(z) k_x^s \tag{5b}$$

$$\gamma_{xz} = g(z) \gamma_{xz}^s \tag{5b}$$

where

$$\varepsilon_x^0 = \frac{\partial u_0}{\partial x}, k_x^b = -\frac{\partial^2 w_b}{\partial x^2}, k_x^s = -\frac{\partial^2 w_s}{\partial x^2}, \gamma_{xz}^s = \frac{\partial w_s}{\partial x} \tag{5c}$$

$$g(z) = 1 - f'(z) = \frac{5}{4} - \frac{5z^2}{h^2} \tag{5d}$$

The state of stress in the beam is given by the generalized Hooke’s law as follows:

$$\sigma_x = Q_{11}(x, z) \varepsilon_x \tag{6a}$$

and

$$\tau_{xz} = Q_{55}(x, z) \gamma_{xz} \tag{6b}$$

where

$$Q_{11}(x, z) = \frac{E(x, z)}{1-\nu^2} \text{ and } Q_{55}(x, z) = \frac{E(x, z)}{2(1+\nu)} \quad (7)$$

2.2 Equations of motion

The equation of motion was derived by employing Hamilton's principle as given by (Şimşek 2009)

$$\delta \int_{t_1}^{t_2} (U - K) dt = 0 \quad (8)$$

where t is the time, t_1 and t_2 are the initial and end time, respectively, δU and δK are the virtual variation of the strain energy and kinetic energy. The variation of the strain energy of the beam can be stated as

$$\begin{aligned} \delta U &= \int_0^L \int_{-\frac{h}{2}}^{\frac{h}{2}} (\sigma_x \delta \varepsilon_x + \tau_{xz} \delta \gamma_{xz}) dz dx \\ &= \int_0^L \left(N_x \frac{d\delta u_0}{dx} - M_b \frac{d^2 \delta w_b}{dx^2} - M_s \frac{d^2 \delta w_s}{dx^2} + Q_{xz} \frac{d\delta w_s}{dx} \right) dx \end{aligned} \quad (9)$$

where N_x , M_b , M_s and Q_{xz} are the stress resultants defined as

$$(N_x, M_b, M_s) = \int_{-\frac{h}{2}}^{\frac{h}{2}} (1, z, f) \sigma_x dz \quad (10a)$$

and

$$Q_{xz} = \int_{-\frac{h}{2}}^{\frac{h}{2}} g \tau_{xz} dz \quad (10b)$$

The variation of the kinetic energy can be expressed as

$$\begin{aligned} \delta K &= \int_0^L \int_{-\frac{h}{2}}^{\frac{h}{2}} \rho(z) [\dot{u} \delta \dot{u} + \dot{w} \delta \dot{w}] dz dx \\ &= \int_0^L \left\{ I_1 [\dot{u}_0 \delta \dot{u}_0 + (\dot{w}_b + \dot{w}_s)(\delta \dot{w}_b + \delta \dot{w}_s)] - I_2 \left(\dot{u}_0 \frac{d\delta \dot{w}_b}{dx} + \frac{d\dot{w}_b}{dx} \delta \dot{u}_0 \right) \right. \\ &\quad + I_4 \left(\frac{d\dot{w}_b}{dx} \frac{d\delta \dot{w}_b}{dx} \right) - I_3 \left(\dot{u}_0 \frac{d\delta \dot{w}_s}{dx} + \frac{d\dot{w}_s}{dx} \delta \dot{u}_0 \right) + I_6 \left(\frac{d\dot{w}_s}{dx} \frac{d\delta \dot{w}_s}{dx} \right) \\ &\quad \left. + I_5 \left(\frac{d\dot{w}_b}{dx} \frac{d\delta \dot{w}_s}{dx} + \frac{d\dot{w}_s}{dx} \frac{d\delta \dot{w}_b}{dx} \right) \right\} dx \end{aligned} \quad (11)$$

where dot-superscript convention indicates the differentiation with respect to the time variable t , $\rho(z)$ is the mass density, and $(I_1, I_2, I_3, I_4, I_5, I_6)$ are the mass inertias defined as

$$(I_1, I_2, I_3, I_4, I_5, I_6) = \int_{-\frac{h}{2}}^{\frac{h}{2}} (1, z, f, z^2, zf, f^2) \rho(z) dz \quad (12)$$

Substituting the expressions for δU and δK from Eqs. (9) and (11) into Eq. (8) and integrating by parts versus both space and time variables, and collecting the coefficients of δu_0 , δw_b , and δw_s , the following equations of motion of the functionally graded beam are obtained

$$\int_x \left(\frac{dN_x}{dx} = I_0 \ddot{u}_0 - I_1 \frac{d\ddot{w}_b}{dx} - J_1 \frac{d\ddot{w}_s}{dx} \right) \delta u_0 dx = 0 \tag{13a}$$

$$\int_x \left(\frac{d^2 M_b}{dx^2} = I_0 (\ddot{w}_b + \ddot{w}_s) + I_1 \frac{d\ddot{u}_0}{dx} - I_2 \frac{d^2 \ddot{w}_b}{dx^2} - J_2 \frac{d^2 \ddot{w}_s}{dx^2} \right) \delta w_b dx = 0 \tag{13b}$$

$$\int_x \left(\frac{d^2 M_s}{dx^2} + \frac{dQ_{xz}}{dx} = I_0 (\ddot{w}_b + \ddot{w}_s) + J_1 \frac{d\ddot{u}_0}{dx} - J_2 \frac{d^2 \ddot{w}_b}{dx^2} - K_2 \frac{d^2 \ddot{w}_s}{dx^2} \right) \delta w_s dx = 0 \tag{13c}$$

Eq. (13) can be expressed in terms of displacements (u_0, w_b, w_s) by using Eqs. (3), (5), (6) and (10) as follows

$$\int_x \left[A_{11} \frac{\partial^2 u_0}{\partial x^2} - B_{11} \frac{\partial^3 w_b}{\partial x^3} - B_{11}^s \frac{\partial^3 w_s}{\partial x^3} - I_0 \ddot{u}_0 + I_1 \frac{d\ddot{w}_b}{dx} + J_1 \frac{d\ddot{w}_s}{dx} \right] \delta u_0 dx = 0 \tag{14a}$$

$$\int_x \left[B_{11} \frac{\partial^3 u_0}{\partial x^3} - D_{11} \frac{\partial^4 w_b}{\partial x^4} - D_{11}^s \frac{\partial^4 w_s}{\partial x^4} - I_0 (\ddot{w}_b + \ddot{w}_s) - I_1 \frac{d\ddot{u}_0}{dx} + I_2 \frac{d^2 \ddot{w}_b}{dx^2} + J_2 \frac{d^2 \ddot{w}_s}{dx^2} \right] \delta w_b dx = 0 \tag{14b}$$

$$\int_x \left[B_{11}^s \frac{\partial^3 u_0}{\partial x^3} - D_{11}^s \frac{\partial^4 w_b}{\partial x^4} - H_{11}^s \frac{\partial^4 w_s}{\partial x^4} + A_{55}^s \frac{\partial^2 w_s}{\partial x^2} - I_0 (\ddot{w}_b + \ddot{w}_s) - J_1 \frac{d\ddot{u}_0}{dx} + J_2 \frac{d^2 \ddot{w}_b}{dx^2} + K_2 \frac{d^2 \ddot{w}_s}{dx^2} \right] \delta w_s dx = 0 \tag{14c}$$

Where A_{11}, D_{11} , etc., are the beam stiffness, defined by

$$(A_{11}, B_{11}, D_{11}, B_{11}^s, D_{11}^s, H_{11}^s) = \int_{-\frac{h}{2}}^{\frac{h}{2}} Q_{11}(1, z, z^2, f(z), z f(z), f^2(z)) dz \tag{15a}$$

and

$$A_{55}^s = \int_{-\frac{h}{2}}^{\frac{h}{2}} Q_{55}[g(z)]^2 dz \tag{15b}$$

2.3 Analytical solution

The equations of motion admit the Navier solutions for simply supported beams. The variables u_0, w_b, w_s can be written by assuming the following variations

$$\begin{Bmatrix} u_0 \\ w_b \\ w_s \end{Bmatrix} = \sum_{m=1}^{\infty} \begin{Bmatrix} U_m \cos(\lambda x) e^{i \omega t} \\ W_{bm} \sin(\lambda x) e^{i \omega t} \\ W_{sm} \sin(\lambda x) e^{i \omega t} \end{Bmatrix} \tag{16}$$

Where U_m, W_{bm} , and W_{sm} are arbitrary parameters to be determined, ω is the eigenfrequency associated with m^{th} eigenmode, and $\lambda = m\pi/L$.

Substituting the expansions of u_0, w_b, w_s from Eqs. (16) into the equations of motion Eq. (14), the analytical solutions can be obtained from the following equations

$$\begin{pmatrix} a_{11} & a_{12} & a_{13} \\ a_{12} & a_{22} & a_{23} \\ a_{13} & a_{23} & a_{33} \end{pmatrix} - \omega^2 \begin{pmatrix} m_{11} & m_{12} & m_{13} \\ m_{12} & m_{22} & m_{23} \\ m_{13} & m_{23} & m_{33} \end{pmatrix} \begin{Bmatrix} U_m \\ W_{bm} \\ W_{sm} \end{Bmatrix} = \begin{Bmatrix} 0 \\ 0 \\ 0 \end{Bmatrix} \tag{17}$$

Where

$$a_{11} = \int_x A_{11} \lambda^2 dx$$

$$a_{12} = - \int_x B_{11} \lambda^3 dx$$

$$\begin{aligned}
 a_{13} &= - \int_x B_{11}^s \lambda^3 dx \\
 a_{22} &= \int_x D_{11} \lambda^4 dx \\
 a_{23} &= \int_x D_{11}^s \lambda^4 dx \\
 a_{33} &= \int_x (H_{11}^s \lambda^4 + A_{55}^s \lambda^2) dx
 \end{aligned} \tag{18a}$$

And

$$\begin{aligned}
 m_{11} &= \int_x I_0 dx, \\
 m_{12} &= - \int_x I_1 \lambda dx, \\
 m_{22} &= \int_x (I_0 + I_2 \lambda^2) dx, \\
 m_{13} &= - \int_x J_1 \lambda dx, \\
 m_{23} &= \int_x (I_0 + J_2 \lambda^2) dx, \\
 m_{33} &= \int_x (I_0 + K_2 \lambda^2) dx
 \end{aligned} \tag{18b}$$

3. Results and discussion

The validation study was performed for BDFG beams for simply supported boundary conditions. Natural frequency was found for varying grading index n_x . The non-dimensional natural frequencies of unidirectional transverse beams ($n_x = 0$) were compared with those obtained by Benaberrahmane *et al.* (2021), the Timoshenko beam theory (TBT) (Şimşek 2010), and the SDT (Ould Larbi *et al.* 2013). An excellent accuracy of the present method with the reference works was obtained.

The benefit of the present method is that it is simple and can be employed easily in case of a combination of loads as well. The metal-ceramic material is aluminium and alumina whose Young's modulus is 70 GPa and 380 GPa and density is 2702 kg/m³ and 3960 kg/m³.

The frequency is normalized as per the following relation:

$$\bar{\omega} = \frac{\omega L^2}{h} \sqrt{\frac{\rho_m}{E_m}}$$

Table 1 shows the results of the validation in which the results of the present method were compared with those available in the literature for slender and short FG beams.

Table 1 Non-dimensional frequencies $\bar{\omega}$ of unidirectional transverse FG beams ($n_x = 0$)

L/h	Sources	index n_z					
		0	0.5	1	2	5	10
5	Present	5.1527	4.4108	4.9904	3.6264	3.4041	3.2857
	Benaberrahmane <i>et al.</i> (2021)	5.1575	4.4137	3.9926	3.6278	3.4019	3.2820
	Ould Larbi <i>et al.</i> (2013)	5.1529	4.4108	3.9905	3.6263	3.4001	3.2812
	TBT (Şimşek 2010)	5.1527	4.4111	3.9904	3.6264	3.4012	3.2816
20	Present	5.4603	4.6511	4.2051	3.8361	3.6487	3.5393
	Benaberrahmane <i>et al.</i> (2021)	5.4654	4.6543	4.2074	3.8376	3.6492	3.5394
	Ould Larbi <i>et al.</i> (2013)	5.4603	4.6511	4.2051	3.8361	3.6484	3.5389
	TBT (Şimşek 2010)	5.4603	4.6511	4.2051	3.8361	3.6485	3.5390

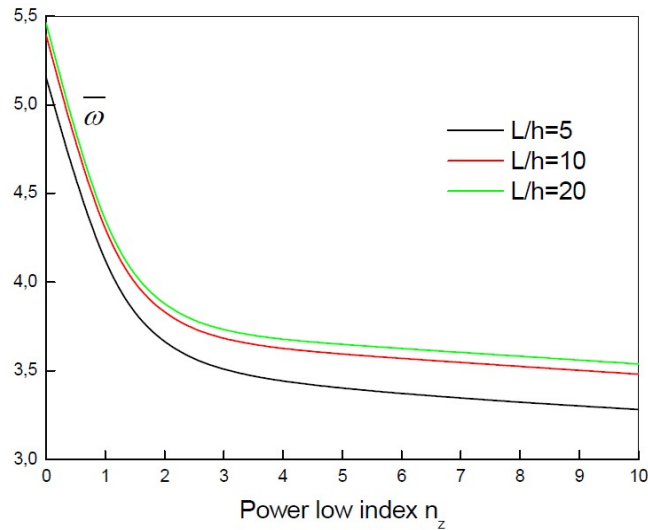


Fig. 3 Variation of the fundamental frequency $\bar{\omega}$ of unidirectional transverse FG beams with power-law index n_z

Table 2 Comparison of non-dimensional frequencies ω^* of simply supported BDFG beam

ω^*	Theories	$n_x = 0$	$n_x = \frac{1}{3}$	$n_x = \frac{1}{2}$	$n_x = \frac{5}{6}$	$n_x = 1$	$n_x = \frac{4}{3}$	$n_x = \frac{3}{2}$	$n_x = 2$
$n_z = 0$	Present	3.3018	3.8217	3.9975	4.2572	4.3562	4.5137	4.5775	4.7282
	Nguyen <i>et al.</i> (2017)	3.3018	3.7429	3.9148	4.1968	4.3139	4.5118	4.5956	4.8005
	Tran and Nguyen (2018)	3.3018	3.7428	3.9146	4.1966	4.3137	4.5116	4.5954	4.8003
	Benaberrahmane <i>et al.</i> (2021)	3.3018	3.5766	3.7793	4.1773	4.3562	4.6653	4.7965	5.1115
$n_z = \frac{1}{3}$	Present	3.1543	3.5681	3.6958	3.8741	3.9389	4.0387	4.0779	4.1681
	Nguyen <i>et al.</i> (2017)	3.1542	3.5050	3.6305	3.8252	3.9022	4.0277	4.0792	4.2009
	Tran and Nguyen (2018)	3.1543	3.5050	3.6305	3.8251	3.9022	4.0276	4.0791	4.2008
	Benaberrahmane <i>et al.</i> (2021)	3.1543	3.3285	3.4880	3.8011	3.9389	4.1705	4.2661	4.488
$n_z = \frac{1}{2}$	Present	3.1070	3.4870	3.6000	3.7548	3.8101	3.8943	3.9271	4.0020
	Nguyen <i>et al.</i> (2017)	3.1068	3.3285	3.5397	3.7087	3.7745	3.8805	3.9236	4.0245
	Tran and Nguyen (2018)	3.1069	3.4285	3.5397	3.7087	3.7745	3.8805	3.9235	4.0244
	Benaberrahmane <i>et al.</i> (2021)	3.1070	3.2481	3.3948	3.6837	3.8101	4.0210	4.1073	4.3058
$n_z = \frac{5}{6}$	Present	3.0506	3.3816	3.4744	3.5974	3.6403	3.7046	3.7293	3.7848
	Nguyen <i>et al.</i> (2017)	3.0504	3.3296	3.4206	3.5548	3.6059	3.6569	3.7194	3.7847
	Tran and Nguyen (2018)	3.0505	3.3296	3.4206	3.5547	3.6058	3.6869	3.7193	3.7946
	Benaberrahmane <i>et al.</i> (2021)	3.0507	3.1431	3.2721	3.5287	3.6403	3.8247	3.8993	4.0687
$n_z = 1$	Present	0.0361	3.3480	3.4333	3.5449	3.5834	3.6409	3.6629	3.7120
	Nguyen <i>et al.</i> (2017)	3.0359	3.2984	3.3819	3.5035	3.5495	3.6219	3.6508	3.7177
	Tran and Nguyen (2018)	3.0359	3.2983	3.3818	3.5034	3.5493	3.6217	3.6507	3.7175
	Benaberrahmane <i>et al.</i> (2021)	3.0362	3.1095	3.2319	3.4771	3.5835	3.7588	3.8295	3.9892

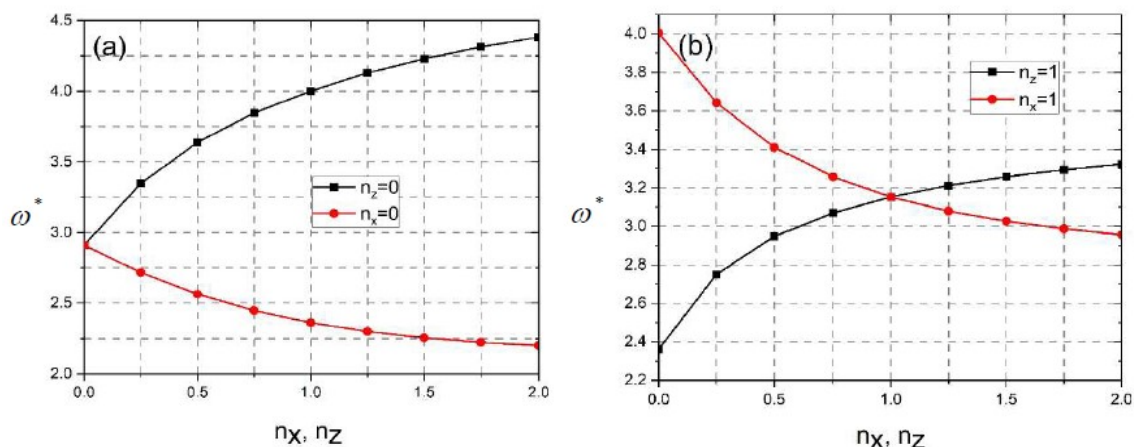


Fig. 4 (a-b) Variation of the non-dimensional frequencies ω^* versus the grading indexes ($L/h=10$)

As indicated in Table 1, it is noted that the results obtained by the present theory demonstrate its reliability compared to other works such as those by Simsek (2010), Ould Larbi *et al.* (2013), Benabderrahmane *et al.* (2021). These theories are considered higher-order theories. Several studies have shown that, compared to classical theory, the results are similar for slender beams, but significant differences arise for thick beams.

Fig. 3 shows the non-dimensional fundamental natural frequency $\bar{\omega}$ of unidirectional transverse FG beams versus the power law index n_z for different values of span-to-depth ratio L/h using the present theory. It is observed that an increase in the value of the power law index leads to a reduction of frequency. The highest frequency values are obtained for full ceramic beams ($n_z = 0$) while the lowest frequency values are obtained for full metal beams ($n_z \rightarrow \infty$). This is due to the fact that an increase in the value of the power law index results in a decrease in the value of the elasticity modulus. In other words, the beam becomes flexible as the power law index increases, thus decreasing the frequency values. It can be also seen that the span-to-depth ratio L/h has a considerable effect on the non-dimensional fundamental natural frequency $\bar{\omega}$ where this latter is reduced with decreasing L/h . This dependence is related to the effect of shear deformation.

Table 3 shows the non-dimensional fundamental frequencies of the BDFG beam for varying power law indices n_x and n_z . In this example a BDFG beam with an aspect ratio $L/h=20$ composed of alumina (Al_2O_3) as ceramic-1, zirconia (ZrO_2) as ceramic-2, SS (SUS304) as metal-1 and Al as metal-2 is used. The following are the properties of the material:

$$\begin{aligned} E_{c1} &= 390 \text{ GPa}, E_{c2} = 200 \text{ GPa}, \\ \rho_{c1} &= 3960 \text{ kg/m}^3, \rho_{c2} = 5700 \text{ kg/m}^3, \\ E_{m1} &= 210 \text{ GPa}, E_{m2} = 70 \text{ GPa}, \\ \rho_{m1} &= 7800 \text{ kg/m}^3, \rho_{m2} = 2702 \text{ kg/m}^3. \end{aligned}$$

The frequencies of the BDFG beam in Table 2 are in the following dimensionless form:

$$\omega^* = \frac{\omega L^2}{h} \sqrt{\frac{\rho_{m2}}{E_{m2}}}$$

Fig. 4(a) and 4(b) show the variation of the dimensionless frequency of BDFG beams as a function of the volume fractions in the two directions n_x and n_z . For Fig. 4(a), both variations start from the same point. This is because it corresponds to the case of the isotropic beam $n_x=n_z=0$. The

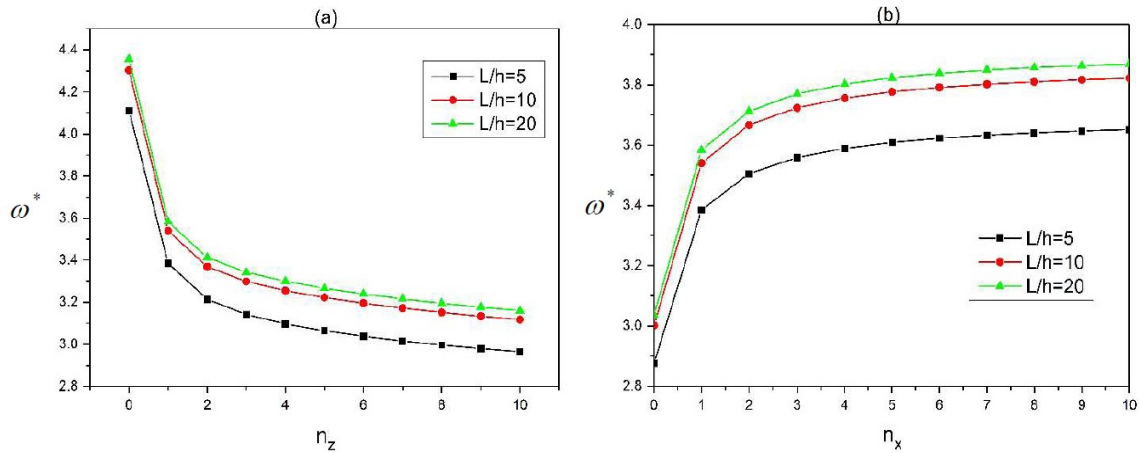


Fig. 5 Variation of the non-dimensional frequencies ω^* versus grading index of BDFG beam simply supported for different ratio L/h ((a) $n_x=1$, (b) $n_z=1$)

case $n_z=0$, has maximum natural frequency as in this case the entire beam is composed of ceramic material. Because of the increase in the stiffness the natural frequency of the beam is higher for a beam with a high ceramic percentage. Increasing the parameter n_x by keeping $n_z=0$, the natural frequency increases, see Fig. 4. On the other hand, keeping $n_x=0$ and increasing n_z a decrease in natural frequency is obtained.

Fabrication of a bi-directional FG beam can be achieved using additive manufacturing techniques and powder metallurgy. To achieve this the fabrication technique of a uni-directional FGM structure can be employed. Thus, for the fabrication of a bi-directional FG structure using powder metallurgy, a powder of two desired material combinations can be stacked and then compressed to a certain pressure. The green compact is then taken to a sintering furnace where it is heated to a certain temperature for a particular duration. The sintered sample then can be tested to check its densification. In both methods, additive manufacturing yields structures with different densification and strength. To obtain a product with high densification an appropriate selection of parameters was required. Because of gradation, the yield strength of a material is also increased which is the same for homogeneous materials. Here, the yield strength is higher in which the composition of ceramic material is higher. Also, Young's modulus is higher for ceramics compared to metals. So, in FGM improved material properties can be achieved by processing the material in a precise manner.

Fig. 5 (a-b) shows the variation of non-dimensional frequency for different L/h ratios and varying index n_x and n_z . The frequency increases with an increase in L/h value and decreases as the parameter n_z increases. On the other hand, the frequency increases with an increase in n_x . It is interesting to note that the frequency is maximum when $n_z=0$ whereas for $n_x=0$, it is minimum. Hence, to obtain the higher frequency the controlling grading parameter is n_x which should be as high as possible keeping the composition of two graded materials in mind. Because in FGMs, the composition of both materials should be there otherwise the component cannot be considered an FG structure.

4. Conclusions

The research demonstrates the importance of bi-directional grading in a functionally graded beam. From the results, it was found that by keeping the grading index $n_z=0$ and then increasing the value of the grading parameter n_x a higher natural frequency can be obtained. A fully ceramic beam has the highest natural frequency but ceramics possess lower toughness values and hence fail when subjected to shock loading. Therefore, reinforcement is added, usually, ceramics are added to the metal phase (matrix) because of the higher melting temperature of ceramics. In this case, the beams are meant only to resist wear and high-temperature resistance rather than a combination of ceramics with high fracture toughness and thermal shock resistance. From the results, it can be concluded that an axial gradation is more beneficial relatively than gradation along thickness. Considering the differences in thermo-mechanical behavior, it is essential to determine the parameters experimentally for each phase due to significant variations in material properties influenced by factors such as chemical composition, microstructure, and processing conditions. Such studies can be exploited as this would enable precise characterization and better consideration of individual material behaviors, thereby enhancing the accuracy and reliability of model predictions, especially under complex loading conditions or at elevated temperatures.

References

- Abdalla, H.M.A., Casagrande, D., De Bona, F., De Monte, T., Sortino, M. and Totis, G. (2021), "An optimized pressure vessel obtained by metal additive manufacturing: Preliminary results", *Int. J. Press. Ves. Pip.*, **192**, 104434. <https://doi.org/10.1016/j.ijpvp.2021.104434>.
- Ait Atmane, R., Mahmoudi, N. and Bennai, R. (2021), "Investigation on the dynamic response of porous FGM beams resting on variable foundation using a new higher order shear deformation theory", *Steel Compos. Struct.*, **39**(1), 95-107. <https://doi.org/10.12989/scs.2021.39.1.095>.
- Akinwamide, S.O., Abe, B.T., Akinribide, O.J., Obadele, B.A. and Olubambi, P.A. (2020), "Characterization of microstructure, mechanical properties and corrosion response of aluminium-based composites fabricated via casting-A review", *Int. J. Adv. Manuf. Technol.*, **109**, 975-991. <https://doi.org/10.1007/s00170-020-05703-1>.
- Ansari, M., Jabari, E. and Toyserkani, E. (2021), "Opportunities and challenges in additive manufacturing of functionally graded metallic materials via powder-fed laser directed energy deposition: A review", *J. Mater. Proc. Technol.*, **294**, 117117. <https://doi.org/10.1016/j.jmatprotec.2021.117117>.
- Avcar, M. (2019), "Free vibration of imperfect sigmoid and power law functionally graded beams", *Steel Compos. Struct.*, **30**(6), 603-615. <https://doi.org/10.12989/scs.2019.30.6.603>.
- Ayache, B., Bennai, R., Fahsi, B., Fourn, H., Ait Atmane, H. and Tounsi, A. (2018), "Analysis of wave propagation and free vibration of functionally graded porous material beam with a novel four variable refined theory", *Earthq. Struct.*, **15**(4), 369-382. <https://doi.org/10.12989/eas.2018.15.4.369>.
- Aydogdu, M. and Taskin, V. (2007), "Free vibration analysis of functionally graded beams with simply supported edges", *Mater. Des.*, **28**(5), 1651-1656. <https://doi.org/10.1016/j.matdes.2006.02.007>.
- Beheshti-Aval, S.B. and Lezgy-Nazargah, M. (2012), "A coupled refined high-order global-local theory and finite element model for static electromechanical response of smart multilayered/sandwich beams", *Arch. Appl. Mech.*, **82**(12), 1709-1752. <https://doi.org/10.1007/s00419-012-0621-9>.
- Benaberrahmane, I., Benyoucef, S., Sekkal, M., Mekerbi, M., Bouiadjra, R.B., Selim, M.M. and Hussain, M. (2021), "Investigating of free vibration behavior of bidirectional FG beams resting on variable elastic foundation", *Geomech. Eng.*, **25**(5), 383-394. <https://doi.org/10.12989/gae.2021.25.5.383>.
- Benferhat, R., Hassaine Daouadji, T., Said Mansour, M. and Hadji, L. (2016), "Free vibration analysis of FG

- plates resting on the elastic foundation and based on the neutral surface concept using higher order shear deformation theory”, *Earthq. Struct.*, **10**(5), 1033-1048. <https://doi.org/10.12989/eas.2016.10.5.1033>.
- Benkhellat, S., Kada, O., Seghir, A. and Kadri, M. (2021), “Seismic damage assessment of reinforced concrete grain silos”, *Int. J. Struct. Stab. Dyn.*, **22**(01), 2250005. <https://doi.org/10.1142/S0219455422500055>.
- Bennai, R., Ait Atmane, R., Bernard, F., Nebab, M., Mahmoudi, N., Ait Atmane, H., Aldosari, S.M. and Tounsi, A. (2022), “Study on stability and free vibration behavior of porous FGM beams”, *Steel Compos. Struct.*, **45**(1), 67-82. <https://doi.org/10.12989/scs.2022.45.1.067>.
- Benoit, M.J., Mazur, M., Easton, M.A. and Brandt, M. (2021), “Effect of alloy composition and laser powder bed fusion parameters on the defect formation and mechanical properties of Inconel 625”, *Int. J. Adv. Manuf. Technol.*, **114**, 915-927. <https://doi.org/10.1007/s00170-021-06957-z>.
- Dahmane, M., Benadouda, M., Bennai, R., Saimi, A. and Ait Atmane, H. (2024), “Effect of crack on the dynamic response of bidirectional porous functionally graded beams on an elastic foundation based on finite element method”, *Acta Mechanica*, **235**(6), 3849-3860. <https://doi.org/10.1007/s00707-024-03906-1>.
- Fenjan, R.M., Ahmed, R.A., Hamad, L.B. and Faleh, N.M. (2020), “A review of numerical approach for dynamic response of strain gradient metal foam shells under constant velocity moving loads”, *Adv. Comput. Des.*, **5**(4), 349-362. <https://doi.org/10.12989/acd.2020.5.4.349>.
- Frahli, H., Bennai, R., Nebab, M., Ait Atmane, H. and Tounsi, A. (2023), “Assessing effects of parameters of viscoelastic foundation on the dynamic response of functionally graded plates using a novel HSDT theory”, *Mech. Adv. Mater. Struct.*, **30**(13), 2765-2779. <https://doi.org/10.1080/15376494.2022.2062632>.
- Ghouilem, K., Mehaddene, R., Ghouilem, J., Kadri, M. and Boulifa, D. (2022), “ANSYS modeling interface and creep behavior of concrete matrix on waste glass powder under constant static stress”, *Mater. Today: Proc.*, **49**, 1084-1092. <https://doi.org/10.1016/j.matpr.2021.09.387>.
- Hadji, L. and Avcar, M. (2021), “Free vibration analysis of FG Porous Sandwich Plates under various boundary conditions”, *J. Appl. Comput. Mech.*, **7**(2), 505-519. <https://doi.org/10.22055/JACM.2020.35328.2628>.
- Karamanli, A., Wattanasakulpong, N., Lezgy-Nazargah, M. and Vo, T.P. (2023), “Bending, buckling and free vibration behaviours of 2D functionally graded curved beams”, *Struct.*, **55**, 778-798. <https://doi.org/10.1016/j.istruc.2023.06.052>.
- Kehli, A., Nebab, M., Bennai, R., Ait Atmane, H. and Dahmane, M. (2024), “Dynamic characteristics analysis of functionally graded cracked beams resting on viscoelastic medium using a new quasi-3D HSDT”, *Mech. Adv. Mater. Struct.*, 1-14. <https://doi.org/10.1080/15376494.2024.2326983>.
- Lahdiri, A. and Kadri, M. (2022), “Free vibration behaviour of multi-directional functionally graded imperfect plates using 3D isogeometric approach”, *Earthq. Struct.*, **22**(5), 538. <https://doi.org/10.12989/eas.2022.22.5.538>.
- Latroch, N., Dahmane, M., Benosman, A.S., Bennai, R., Ait Atmane, H. and Benadouda, M. (2023), “Inclined crack identification in bidirectional FG beams on an elastic foundation using the h-version of the finite element method”, *Mech. Adv. Mater. Struct.*, 1-7. <https://doi.org/10.1080/15376494.2023.2290226>.
- Lezgy-Nazargah, M. (2015), “Fully coupled thermo-mechanical analysis of bi-directional FGM beams using NURBS isogeometric finite element approach”, *Aerosp. Sci. Technol.*, **45**, 154-164. <https://doi.org/10.1016/j.ast.2015.05.006>.
- Lezgy-Nazargah, M. (2017), “Assessment of refined high-order global–local theory for progressive failure analysis of laminated composite beams”, *Acta Mechanica*, **228**(5), 1923-1940. <https://doi.org/10.1007/s00707-017-1807-6>.
- Lezgy-Nazargah, M., Karamanli, A. and Vo, T.P. (2023), “Bending, buckling and free vibration analyses of shallow-to-deep FG curved sandwich beams using a global–local refined shear deformation theory”, *Struct.*, **52**, 568-581. <https://doi.org/10.1016/j.istruc.2023.04.008>.
- Lezgy-Nazargah, M., Shariyat, M. and Beheshti-Aval, S.B. (2011), “A refined high-order global-local theory for finite element bending and vibration analyses of laminated composite beams”, *Acta Mechanica*, **217**(3), 219-242. <https://doi.org/10.1007/s00707-010-0391-9>.

- Lezgy-Nazargah, M., Trinh, L.C., Wattanasakulpong, N. and Vo, T.P. (2024), "Finite element model for stability and vibration analyses of bi-directional FG curved sandwich beams", *Int. J. Mech. Mater. Des.*, 1-27. <https://doi.org/10.1007/s10999-023-09700-6>.
- Lu, Y. and Chen, X. (2020), "Nonlinear parametric dynamics of bidirectional functionally graded beams", *Shock Vib*, Article ID 8840833, 1-13. <https://doi.org/10.1155/2020/8840833>.
- Madan, R. and Bhowmick, S. (2020), "A review on application of FGM fabricated using solid-state processes", *Adv. Mater. Proc. Technol.*, **6**(3), 608-619. <https://doi.org/10.1080/2374068X.2020.1731153>.
- Madan, R. and Bhowmick, S. (2022), "Modeling of functionally graded materials to estimate effective thermo-mechanical properties", *World J. Eng.*, **19**(3), 291-301. <https://doi.org/10.1108/WJE-09-2020-0445>.
- Madan, R. and Bhowmick, S. (2023), "Fabrication and microstructural characterization of Al-SiC based functionally graded disk", *Aircraft Eng. Aerosp. Technol.*, **95**(2), 292-301. <https://doi.org/10.1108/aeat-03-2022-0096>.
- Mellal, F., Bennai, R., Avcar, M., Nebab, M. and Ait Atmane, H. (2023), "On the vibration and buckling behaviors of porous FG beams resting on variable elastic foundation utilizing higher-order shear deformation theory", *Acta Mechanica*, **234**(9), 3955-3977. <https://doi.org/10.1007/s00707-023-03603-5>.
- Nebab, M., Atmane, H.A., Bennai, R. and Dahmane, M. (2024), "Warping and porosity effects on the mechanical response of FG-Beams on non-homogeneous foundations via a Quasi-3D HSDT", *Struct. Eng. Mech.*, **90**(1), 83-94. <https://doi.org/10.12989/sem.2024.90.1.083>.
- Nakamura, T., Wang, T. and Sampath, S. (2000), "Determination of properties of graded materials by inverse analysis and instrumented indentation", *Acta Materialia*, **48**(17), 4293-4306. [https://doi.org/10.1016/S1359-6454\(00\)00217-2](https://doi.org/10.1016/S1359-6454(00)00217-2).
- Nebab, M., Ait Atmane, H., Bennai, R. and Dahmane, M. (2024), "Warping and porosity effects on the mechanical response of FG-Beams on non-homogeneous foundations via a Quasi-3D HSDT", *Struct. Eng. Mech.*, **90**(1), 83-94. <https://doi.org/10.12989/sem.2024.90.1.083>.
- Nebab, M., Dahmane, M., Belqassim, A., Ait Atmane, H., Bernard, F., Benadouda, M., Bennai, R. and Hadji, L. (2023), "Fundamental frequencies of cracked FGM beams with influence of porosity and Winkler/Pasternak/Kerr foundation support using a new quasi-3D HSDT", *Mech. Adv. Mater. Struct.*, 1-13. <https://doi.org/10.1080/15376494.2023.2294371>.
- Nguyen, D.K., Nguyen, Q.H., Tran, T.T. and Bui, V.T. (2017), "Vibration of bi-dimensional functionally graded Timoshenko beams excited by a moving load", *Acta Mechanica*, **228**, 141-155. <https://doi.org/10.1007/s00707-016-1705-3>.
- Norio, H., Hideaki, I. and Takuji, N. (1992), "Stress intensity factors of cracks initiating from a rhombic hole due to uniform heat flux", *Eng. Fract. Mech.*, **42**(2), 331-337. [https://doi.org/10.1016/0013-7944\(92\)90223-2](https://doi.org/10.1016/0013-7944(92)90223-2).
- Ould Larbi, L., Kaci, A., Houari, M.S.A. and Tounsi, A. (2013), "An efficient shear deformation beam theory based on neutral surface position for bending and free vibration of functionally graded beams", *Mech. Bas. Des. Struct. Mach.*, **41**(4), 421-433. <https://doi.org/10.1080/15397734.2013.763713>.
- Rabahi, A., Hassaine Daouadji, T. and Benferhat, R. (2021), "Modeling and analysis of the imperfect FGM-damaged RC hybrid beams", *Adv. Comput. Des.*, **6**(2), 117-133. <https://doi.org/10.12989/acd.2021.6.2.117>.
- Sankar, B.V. (2001), "An elasticity solution for functionally graded beams", *Compos. Sci. Technol.*, **61**(5), 689-696. [https://doi.org/10.1016/S0266-3538\(01\)00007-0](https://doi.org/10.1016/S0266-3538(01)00007-0).
- Şimşek, M. (2010), "Fundamental frequency analysis of functionally graded beams by using different higher-order beam theories", *Nucl. Eng. Des.*, **240**(4), 697-705. <https://doi.org/10.1016/j.nucengdes.2009.12.013>.
- Singh, A. and Kumari, P. (2020), "Analytical free vibration solution for angle-ply piezolaminated plate under cylindrical bending: A piezo-elasticity approach", *Adv. Comput. Des.*, **5**(1), 55-89. <https://doi.org/10.12989/acd.2020.5.1.055>.
- Thai, H.T. and Vo, T.P. (2012), "Bending and free vibration of functionally graded beams using various higher-order shear deformation beam theories", *Int. J. Mech. Sci.*, **62**(1), 57-66.

<https://doi.org/10.1016/j.ijmecsci.2012.05.014>.

Thom, T.T. and Kien, N.D. (2018), "Free vibration analysis of 2-D FGM beams in thermal environment based on a new third-order shear deformation theory", *Vietnam J. Mech.*, **40**(2), 121-140. <https://doi.org/10.15625/0866-7136/10503>.

Verma, R.K., Parganiha, D. and Chopkar, M. (2021), "A review on fabrication and characteristics of functionally graded aluminum matrix composites fabricated by centrifugal casting method", *SN Appl. Sci.*, **3**, 227. <https://doi.org/10.1007/s42452-021-04200-8>.

Ying, J., Lü, C.F. and Chen, W.Q. (2008), "Two-dimensional elasticity solutions for functionally graded beams resting on elastic foundations", *Compos. Struct.*, **84**(3), 209-219. <https://doi.org/10.1016/j.compstruct.2007.07.004>.

CC